

# Quality evaluation of apples based on surface defects: development of an automated inspection system

J.A. Throop<sup>a,\*</sup>, D.J. Aneshansley<sup>a</sup>, W.C. Anger<sup>b</sup>, D.L. Peterson<sup>b</sup>

<sup>a</sup> Cornell University, Department of Biological and Environmental Engineering, Ithaca, NY 14853, USA

<sup>b</sup> USDA-ARS Appalachian Fruit Research Station Kearneysville, WV 25430, USA

Received 7 May 2004; accepted 15 January 2005

## Abstract

The development of an automated inspection station to grade processing apples includes a conveyor for apple orientation, optics and camera to capture identical images at three predetermined wavebands, a lighting system that illuminates the apple's surface diffusely and image processing algorithms to segment surface defects on apples in real time.

The conveyor oriented apples so that the stem/calyx ends were not visible during image capture. Multi-spectral optics fabricated using a multi-vision linear filter mounted in front of the camera lens provided three different waveband (740, 950 nm and visible) images of apples on a single camera array. Interference filters placed in the optical path provided the different wavebands.

The diameter and height of each apple was measured to estimate the apple's volume. These dimensions and the position of the apple in the image allowed a portion of each image to be defined, the so-called region of interest (ROI). These sub-images made a composite image of the apple's surface.

© 2005 Elsevier B.V. All rights reserved.

**Keywords:** Apples; Apple grading; Automated inspection; Apple sorting; Defects; Defect detection

## 1. Introduction

Sorting machines generally convey apples on bi-cone rollers without knowledge of location of the stem/calyx ends. With the exception of Washington State grown Red Delicious, bi-cone rollers failed to orient apples better than 90% of the time (Throop et al., 1995, 1997, 2001).

Image processing techniques have been tested to assure that stems and calyxes would not be counted as defects (Crowe and Delwiche, 1996; Campins et al., 1997; Yang, 1996; Penman, 2001; Li et al., 2002). An alternate solution is to orient the stem and calyx to a known position. The first application of conveyed and oriented apples was for peeling and coring during processing (Keesling, 1965; Tichy, 1988; Ross et al., 1996). Orientation of apples was also used on a commercial color sorter (VanderSchoot, 1994).

Spectral reflectance can be used to detect surface defects. Aneshansley et al. (1997) examined the re-

\* Corresponding author. Tel.: +1 607 255 8464; fax: +1 607 255 4080.

E-mail address: [jat12@cornell.edu](mailto:jat12@cornell.edu) (J.A. Throop).

flectance spectra for 21 different surface defects for wavelengths between 460 and 1030 nm. Statistical processing of the data from damaged and undamaged areas on the apple identified three wavelength bands (540, 750 and 950 nm), at least one of which produced the best image contrast for each of the 21 defects. Throop et al. (1999, 2000) described a multi-spectral inspection station that captured images of apple reflectance for four wavebands (540, 650, 750 and 950 nm) that required pre-sizing of apples before inspection.

### 1.1. Inspection of apples for processing

Typically, when a truckload of apples arrives at a processing plant, a random sample of 300–500 apples is taken. Based on the weight, damage and size of apples found in this sample, the grower is paid accordingly for the whole truckload (USDA Agricultural Marketing Services, 1997).

USDA standards for US No. 1 and US No. 2 limits cut waste to no more than 5 and 12%, respectively, of total volume. More than 12% cut waste is classified as cider/cull. Throop et al. (2000) calculated “waste” volume from the areas of defects and apple volume from apple diameter on 959 apples. Defects on the skin surface such as sooty blotch, fly speck and russet caused 58 of 959 (6.0%) apples to be downgraded to either US No. 2 or cider/cull. 2.9% were downgraded because of incorrect size or improper placement of the apple with respect to the defined region of interest during image capture. 2.6% failed to hold orientation even after being placed on the conveyor in an oriented position. The camera failed to see bruising for six apples (0.6%) and two apples failed to rotate.

### 1.2. Objectives

- (1) Measure apple size to determine the height and width, and position in the image. From this information, smaller sub-images are produced. These sub-images are combined into a composite image representing the apple surface.
- (2) Design a lighting system that radiates only the desired wavelength bands with adjustable intensity controls eliminating the need for neutral density filters to normalize the camera sensor’s response and reduce cooling requirements.

- (3) Based on apple size select a correspondingly sized white reference to flat-field correct apple images before image processing.
- (4) Design special optics to produce different waveband images simultaneously on a common pixel array without chromatic aberration.
- (5) Design a conveying system that orients the stem/calyx regions out of the camera’s view regardless of apple’s shape or cultivar.

## 2. Materials and methods

The inspection station described includes five areas: (1) orientation and presentation, (2) lighting, (3) special optics, (4) image capture and (5) image processing.

### 2.1. Orientation and presentation

The conveyor used for orientation and presentation has been described (Throop et al., 2003). Orientation occurs as an apple sits on top of a rotating wheel whose opposite side contacts a continuously moving flat belt. The concave shape of the stem/calyx regions causes the apple to lose contact with the wheel leaving the apple oriented with the stem/calyx axis vertical. The apple is tipped out of the cup by two concentric rings to an angle of 45° and supported on one side by a pair of cylindrical rollers that rotate the apple during image capture exposing the apple surface for lighting and viewing (Figs. 1 and 2). After image capture, the process is reversed and the apple exits the conveyor. The conveyor is 4.27 m long, using 3.25 m of the length for orientation and moves 0.508 m s<sup>-1</sup> allowing 6.4 s for apple orientation. Apple image capture and processing rate is five apples per second.

### 2.2. Lighting

Four panels of light emitting diodes (LED) were constructed using multiple rows of diodes. Two side panels (35.6 cm × 12.7 cm) consisted of nine rows of 24 LEDs and two smaller panels (18.4 cm × 15.2 cm) consisted of nine rows of 12 LEDs. The 740 nm (ELD-740-524, Roithner Lasertechnik, A-1040 Vienna, Austria, Schoenbrunner Strasse 7) and 950 nm (ELD-950-545, Roithner Lasertechnik, A-1040 Vienna, Austria,

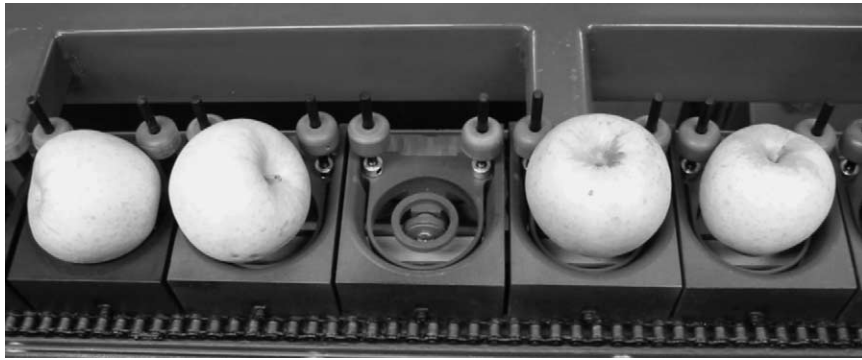


Fig. 1. Overhead view of conveyor designed for orienting apples to capture images to detect surface defects with two apples on the right in an oriented position.

Schoenbrunner Strasse 7) LEDs were alternated in each row and mounted in holes spaced on 12.7 mm centers punched through 0.64 mm thick anodized aluminum sheeting (Coilzak Diffuse, Southco Metal Services, Norcross, GA 30071). Five adjustable current limiting resistors controlled the intensity of rows 1 and 9, 2 and 8, 3 and 7, 4 and 6, and row 5, respectively. A 6.35 mm thick polypropylene (AIN Plastics,

Mt. Vernon, NY 10550) diffuser was placed in front of each side panel and was mounted parallel to the flow of apples. The light was directed upward and across the conveyor to a curved reflector of flat-white painted aluminum, focusing light onto the top or bottom of the tipped apples (Fig. 2). Two smaller panels were mounted above and perpendicular to apple flow and angled down at about 45°. They were fo-



Fig. 2. The light from each side panel reflected from a reflector onto the apple surface. The small panel in the center at the apple exit and a similar one at the apple entrance to the field of view provide additional light at the ends of the side panels.

cused at the entrance and exit of the camera's field of view.

### 2.3. Special optics

A new optical system that projects three identical images for three wavebands simultaneously onto a common camera array has been previously described (Aneshansley et al., 2003). The field of view projected onto the camera array was determined by the lens selected, distance from the camera array to the back of the 25 mm lens, the camera array size, the length of the filter extension tube and the distance of the camera from the object. In this case, the 406.4 mm field of view nearly covers the height of the 1024 pixel  $\times$  1024 pixel array in the camera at a distance of 876 mm between the front of the camera lens and the surface of the apples on the conveyor.

### 2.4. Image capture

The image capture system included a scientific grade digital camera (SMD-1M60, Silicon Mountain Design, Colorado Springs, CO), an image capture card with 4 Mb VRAM (Raptor, Bitflow Inc., Woburn, MA) inserted into a 533 MHz clocked 21164A Alpha processor equipped desktop computer (Aspen Systems Inc., Wheat Ridge, CO) (Throop et al., 2000). Image processing software was a custom version of QUANTIM software (ZEDEC Technologies, Morrisville, NC).

Regions of interest (ROI) are initially set by centering a rectangle within an image of a hardwood sphere run through the field of view prior to image capture of apples. The spheres were 88.9 mm in diameter and painted flat-white. The pixel height, pixel width and center location of a rectangle that fits within the boundaries of the sphere's image is used to size and locate the ROI. The apple rotational speed is adjusted for one revolution of the sphere as six views of the ROI are captured while the sphere passes through the camera's field of view.

A pair of reflective photoelectric sensors (E3G-L11, Omron Electronics, Schaumburg, IL 60173) mounted perpendicular to the conveyor and spaced halfway between conveyor flights (50.8 mm) is triggered by the flight's leading edge to provide an external trigger to the camera.

### 2.5. Image processing

Seven images are captured of each apple while passing through the camera's field of view and three apples can be in the field of view at the same time (Figs. 3 and 4).

#### 2.5.1. Sizing the apple

The first image, a side view of the apple, is segmented from the background and the apple diameter and apple area are found. The apple height using area of ellipse (apple area) and the major axis (apple diameter) is then determined. The rotational speed of the cylindrical rollers in combination with the conveyor travel speed are set to get one complete revolution from the second to the seventh image for an 88.9 mm reference sphere. For smaller apple diameters, this set ROI height includes more than one-sixth of the circumference, so fewer than six ROI represent the total apple surface. The ratio of the smaller apple diameter to the reference sphere's diameter multiplied times the total pixel rows of the reference sphere's circumference gives the exact number of pixel rows representing one complete rotation of any smaller apple. In a similar manner, the width in pixels of the new ROI for smaller apples can be found by finding the ratio of the smaller apple's height to the height of the reference sphere and multiplying this ratio times the height of the reference sphere in pixels. By this method, the camera is always capturing more information than is required and down sizing each ROI and adjusting the total number of pixel rows representing one revolution of an apple. Fig. 5A shows the image with oversized ROI as captured. Fig. 5B shows the resulting image after processing with the adjusted ROI size and with bruises segmented as defects.

#### 2.5.2. Flat-field correction

A prerecorded image of a reference sphere (diameters of 63.5, 69.9, 76.2, 82.6 or 88.9 mm) closest to the apple's diameter, and with a maximum intensity of 200 gray levels, is selected. The image pixel values are subtracted from 255 gray levels and added to the apple image.

#### 2.5.3. Process 740 and 950 nm ROI not used

Preset gray levels for 740 and 950 nm images are used to segment surface defects. The user can select a few apples with typical defects and run them through



Fig. 3. Special optics attached to the camera by a custom extension, a multi-vision linear filter and interference filters.

the inspection process. The images after processing can be viewed. The threshold values can be manually adjusted and the images reprocessed by clicking the re-process button until the desired segmentation occurs.

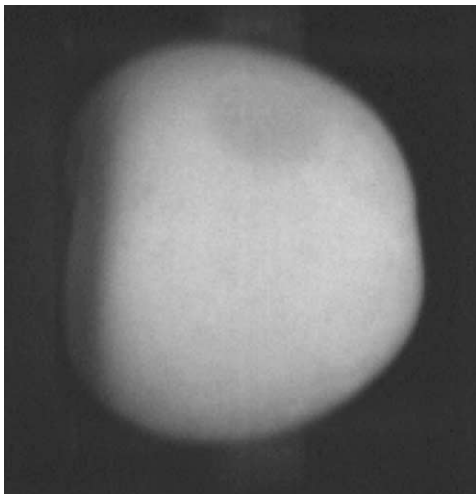


Fig. 4. The first of seven views of a Golden Delicious apple captured as the apple passes through the camera field of view. Apple diameter and total area are measured to calculate ROI size during image processing.

The 740 nm ROI is normalized to the 950 nm ROI based on measured average gray level and the normalized 740 nm ROI is subtracted from the 950 nm ROI with a 128 gray level offset. (The offset prevents the resultant from ever being negative.) A user set threshold level segments defects with reflectance greater than undamaged tissue. The above process is repeated for each ROI. When the running sum of pixel height of the processed ROI equals the computed total pixels representing one apple rotation, processing stops. A logical OR operation places all segmented defects for each waveband view into one image. Bruise volume is computed as cut waste and used to classify the apple into one of three grades, US No. 1, US No. 2, cider/cull (Throop et al., 2000).

### 3. Results and discussion

#### 3.1. Orientation

A total of 1201 apples from 14 cultivars were tested with 28 apples or 2.3% failing to orient (Table 1) the first time through the machine. Apples that failed to ori-

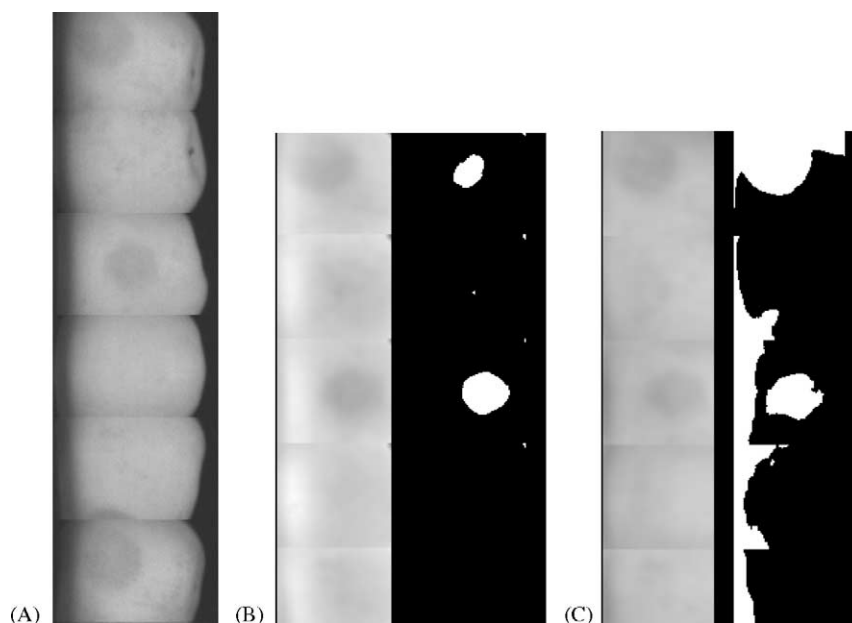


Fig. 5. Images two to seven are captured as oversized ROI and are resized during processing from measurements made from the first image (A). The processed image with resized ROI based on measured apple height and width representing one rotation and flat-field corrected using an image of a flat white sphere 69.9 mm diameter (B). Same image processed using an image of an 88.9 mm diameter flat-white wooden sphere for flat-field correction does not remove edge effects (C).

ent were placed in the machine a second time with 20 of the 28 apples orienting. Apples that failed were evenly scattered between the largest and smallest apple diameter oriented, 92.7 and 59.2 mm, respectively. All ap-

ples that oriented were tipped by the flight mechanism to 45° and rotated correctly on the cylindrical rollers that contacted the side of the apple while in front of the camera (Fig. 2). The two concentric rings, designed to

Table 1

List of cultivars tested on surface defect flight conveyor including the number of apples tested, percent and the largest and smallest diameter apple that oriented and the number of apples that failed to orient the first and second try

Cultivar	Total no.	Percent oriented	Largest diameter/height (mm)	Smallest diameter/height (mm)	Fail first run	Fail second run
McIntosh	80	96.3	87.6/64.5	71.1/54.1	3	1
Suncrisp	80	96.3	90.2/80.0	62.0/48.26	3	0
Braeburn	80	100.0	85.9/78.2	64.8/51.1	0	0
Gala	80	96.3	73.4/64.8	66.3/59.9	3	1
Romes	88	97.7	90.9/75.2	72.4/58.9	2	0
Jonagold	88	96.6	91.2/75.9	71.4/63.0	3	1
Stayman	85	95.3	92.7/75.4	70.1/55.6	4	2
Granny Smith	88	95.5	89.4/74.9	69.9/57.2	4	0
Red Delicious	88	98.9	84.3/71.1	68.6/54.9	1	1
Empire	92	97.8	86.1/72.6	62.7/47.2	2	0
Red Fuji	88	100	87.1/64.5	62.2/53.1	0	0
Enterprize	88	97.7	90.9/78.2	67.8/55.6	2	1
Fuji	88	98.9	90.2/76.7	59.2/49.8	1	1
Pink Lady	88	100	88.6/82.6	67.3/63.8	0	0
Total	1201				28	8

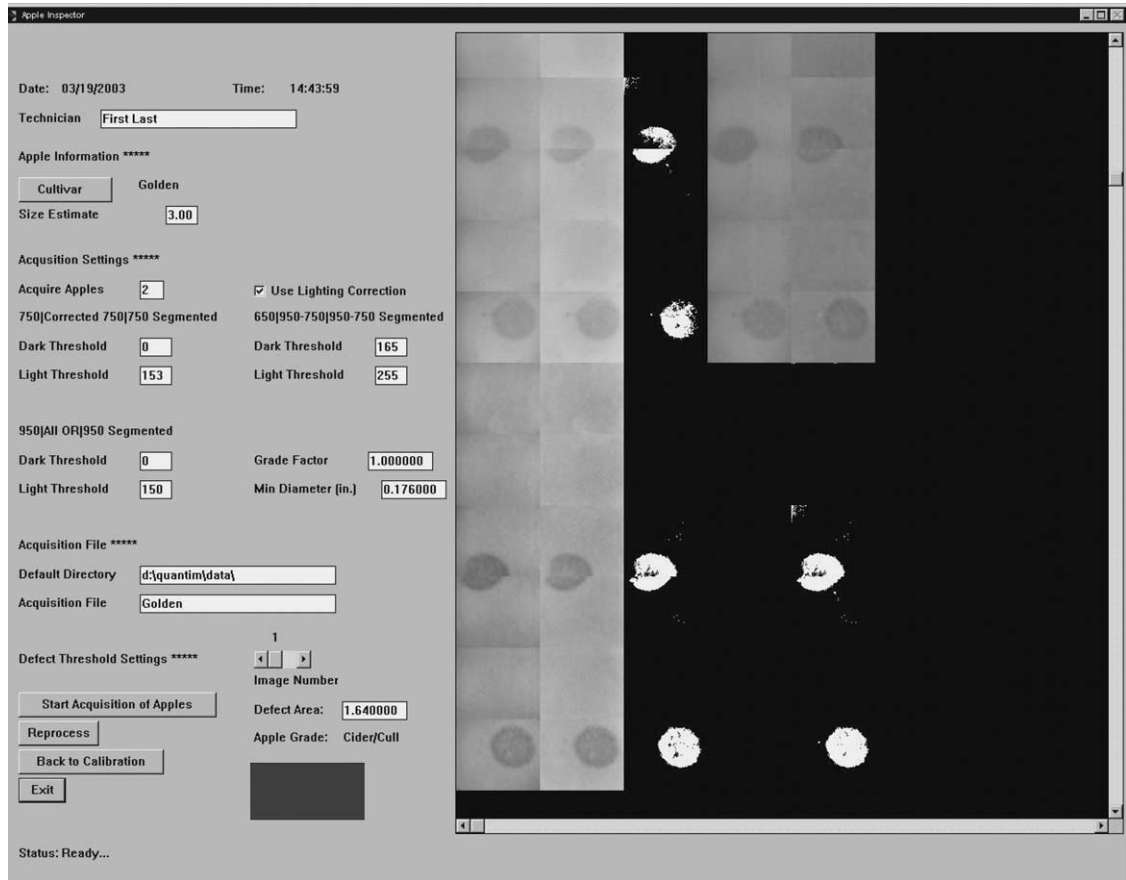


Fig. 6. Computer output screen for viewing each processed apple image and the resulting grade classification. The apple surface in the upper left-to-right views include: the 740 nm waveband before flat-field correction, 740 nm waveband flat-field corrected, segmented 740 nm view, future color view, 740 nm view subtracted from 950 nm waveband image and segmented 950–740 nm. Lower views left-to-right include: the 950 nm waveband before flat-field correction, 950 nm waveband after flat-field correction, segmented 950 nm view and logical OR of all segmented views.

support the apple over the wheel rotating during orientation, allowed stems to move without catching on the mechanism.

### 3.2. Special optics

The multi-vision linear filter showed no chromatic aberrations with wavebands of 540, 740 and 950 nm resulting in images captured for each waveband that were all in focus at a common setting. The interference filters had to be carefully placed in the holder without any visible space between filters and the filter edges had to be painted black to prevent unwanted reflections (Throop et al., 2003).

### 3.3. LED lighting

Reflectors had to be added to the side panels to diffuse the light further by increasing the length of the light path and better diffusing the light produced by each LED (Fig. 2). The intensity adjustment for LED rows corrected for geometric reflectance variations caused by the spherical shape of each apple. The heating that occurred with the previous incandescent lighting was eliminated. The LED lighting has a life span greater than 20,000 h with no noticeable decay in output with age. This compares with the incandescent lighting that had a continual decay with a 750-h life span.

### 3.4. Sphere size and flat-field correction

Fig. 5A shows an unprocessed 71 mm diameter Golden Delicious apple image. Fig. 5B and C shows flat-field corrected views of the Golden Delicious image using prerecorded white hardwood sphere images with diameters of 69.9 and 88.9 mm, respectively. Using equal threshold values, the dark areas in the left side of the unprocessed image are eliminated when using a corresponding size flat-white sphere for flat-field correction (Fig. 5B). It was observed that a choice from three sphere sizes, 69.9, 78 and 88.9 mm, was adequate for flat-field correction instead of using five as tested.

### 3.5. Output screen showing results

Fig. 6 shows the output screen where the six ROI are displayed adjacent to each other. The apple surface in the upper left-to-right views include the 740 nm waveband before flat-field correction, 740 nm waveband flat-field corrected, segmented 740 nm view, future color view, 740 nm view subtracted from 950 nm waveband image and segmented 950–740 nm. Lower views left-to-right include the 950 nm waveband before flat-field correction, 950 nm waveband after flat-field correction, segmented 950 nm view and logical OR of all segmented views. The dark and light threshold values can be adjusted for each waveband segmented and

an image can be reprocessed with the new threshold values by clicking a reprocess button. The minimum defect area to be counted for each segmented cluster of white pixels can be set and the total area of all counted clusters is displayed as the total defect area. The grade factor is a multiplier times each defect area that along with adjusting the segmenting thresholds can be used to adjust the sensitivity of the final grade classification. The total defect area is displayed in square inches. Apples are classified into three apple processing grades, US No. 1, US No. 2 and cull/cider, based on a calculated cut volume using each measured defect area >1.46 cm (Throop et al., 2000). The rectangular box below apple grade is used to indicate by color apple processing grade: shows green for US No. 1, yellow for US No. 2 and red for cider/cull. All defect sizes and the grade for each apple were saved to a file for future reference.

### 3.6. Effect of improvements

Table 2 shows the number of apples misclassified for a test of 959 apples using an inspection system with a different conveyor, lighting and optical system (Throop et al., 2000). The new conveyor design with placement of the stem or calyx on a fixed plane during rotation visibly decreased image processing errors associated with orientation, wobble and placement of the ROI. The procedure for measuring each apple and

Table 2

Shows the number out of a 959 apple sample downgraded due to poor orientation, incorrect size and placement of the ROI, russet and sooty blotch blocking viewing of other defects and upgrading of apples because of failure to sense bruising or lack of apple rotation (Throop et al., 2000)

Cultivar	Poor orientation	ROI incorrect	ROI placement	Russet/SootyBlotch	Missed bruising	Failed to rotate
Golden Delicious	4	0	0	32	2	0
Golden Delicious	1	0	0	9	0	2
Grimes	2	3	0	0	1	0
Empire	1	1	0	0	0	0
Empire	0	0	0	0	1	0
Fuji	6	0	9	0	0	0
Golden Delicious	0	1	0	6	0	0
Golden Delicious	1	3	0	3	1	0
Jonagold	9	0	0	0	0	0
Rome	0	0	3	5	0	0
Golden Delicious	1	4	0	2	1	0
Stayman	0	0	0	0	0	0
Stayman	0	0	0	0	0	0
Stayman	0	1	0	0	0	0
Total	25	13	12	58	6	2

adjusting the size of the ROI according to this measurement decreased the errors associated with incorrect sizing of the ROI. The grading error represented in Table 2 is 12% of the 959 apples tested and required more than a year for testing. Improved spraying applications to counter sooty blotch, russet and flyspeck outbreaks, the misclassification of apples would be expected to be near 6%. The changes in conveyor operation would decrease orientation errors from 2.8 to 2.4%. This is significant when you consider that the 2.8% error was for apples placed on the conveyor already oriented. The changes in lighting and optics will decrease error but have not been quantified. However, it is expected that misclassification of apples with the improved system would be less than 5%. The USDA Grading Standards for processed apples typically allow a 10% error. The misclassification by USDA graders is unknown.

#### 4. Conclusions

The described inspection station was designed for processed apples and included pre-sizing, LED lighting, flat-field correction based on apple size, special optics for multi-spectral image capture and a handling system that oriented all cultivars with a success rate greater than 97.6%.

- (1) *Pre-sizing*: A method was shown that measured each apple diameter, area and computed apple height before processing for defects. These measured values were used to set the region of interest and select the appropriate white reference wooden sphere (images of different diameters are used for flat-field correction during image processing). Apple volume was computed from the apple diameter.
- (2) *New lighting*: Lighting panels of alternating LEDs emitting 740 and 950 nm wavebands provided lighting that required no fans to reduce heating and provided a stable light over a long lifetime. Adjustments for each row and waveband of LEDs allowed for camera response and geometric normalization over the camera field of view.
- (3) *Flat-field correction based on apple size*: Three white wooden spheres with diameters of 69.9, 76.2 and 88.9 mm provide adequate choices to correct

geometric, lighting and background variations in the apple's images before processing.

- (4) *New optics*: Special optics allowed three wavebands (540, 740 and 950 nm) of an apple image to be simultaneously captured through a common aperture onto a single camera array. Chromatic aberration was not present allowing all wavebands to be in focus for the same lens setting.
- (5) *Handling system*: The conveyor oriented 1173 out of 1201 apples (97.6%) of 14 different cultivars. Of the 28 apples that failed to orient, 20 correctly oriented during a second pass on the conveyor. The oriented apples had one edge of each apple referenced to a pair of concentric support rings. This provided a fixed reference as each apple rotated during image capture resulting in consistent apple placement with respect to the region of interest. A 4.27 m long conveyor, using 3.25 m of the length for orientation and moving  $0.508 \text{ m s}^{-1}$  allowed 6.4 s for apple orientation. Apple image capture and processing rate was five apples per second.

From previous results for testing the image processing algorithm with the addition of improved orientation, rotation during image capture without wobble and ROI set according to the apple size coupled with improved spraying practices, it is reasonable to expect fewer than 5% misclassification. This is well within the 10% tolerance currently allowed hand grading.

#### Acknowledgements

This project is supported in part by USDA Cooperative Agreement 58-1931-0-028 with the ARS-USDA Appalachian Fruit Research Station, Kearneysville, WV and by the Agricultural Experiment Station at Cornell University with Hatch Regional Project NE179 and NE1008. Special thanks to Scott Wolford (ARS-USDA Appalachian Fruit Research Station) for his ideas, fabrication knowledge and construction skills that made this research possible.

All programs and services of the USDA and Cornell University are offered on a nondiscriminatory basis with regard to race, color, national origin, religion, sex, age, marital status or handicap. Mention of a trademark, or product does not constitute a guarantee, warranty or endorsement of the product.

## References

- Aneshansley, D.J., Throop, J.A., Upchurch, B.L., 1997. Reflectance spectra of surface defects on apples. In: *Proceedings from the Sensors for Nondestructive Testing International Conference*, Orlando, FL, pp. 143–160.
- Aneshansley, D.J., Throop, J.A., Anger, W.C., Peterson, D.L., 2003. A multi-vision linear filter for capturing multi-spectral images. ASAE Paper No. 033027, ASAE, St. Joseph, MI, p. 49085.
- Campins, J., Throop, J.A., Aneshansley, D.J., 1997. Apple stem and calyx identification for automatic sorting. ASAE Paper No. 973079, ASAE, St. Joseph, MI, 49085.
- Crowe, T.G., Delwiche, M.J., 1996. Real-time defect detection in fruit. Part II: an algorithm and performance of a prototype system. *Trans. ASAE* 39, 2309–2317.
- Keesling, T.B., 1965. Fruit processing method. US Patent No. 3,225,892. Commissioner of Patents and Trademarks, Washington, DC, 15 pp.
- Li, Qingzhong, Wang, M., Gu, W., 2002. Computer vision based system for apple surface defect detection. *Comput. Electron. Agric.* 36, 215–223.
- Penman, D.W., 2001. Determination of stem and calyx location on apples using automatic visual inspection. *Comput. Electron. Agric.* 33, 7–18.
- Ross, E.E., Meissner, K.E., 1996. Agitating apple orientor. US Patent No. 5,544,731. Commissioner of Patents and Trademarks, Washington, DC, p. 9.
- Throop, J.A., Aneshansley, D.J., Upchurch, B.L., 1995. Apple orientation on automatic sorting equipment. ASAE Paper No. 956176, ASAE, St. Joseph, MI, p. 49085.
- Throop, J.A., Aneshansley, D.J., Upchurch, B.L., 1997. Apple orientation on automatic sorting equipment. In: *Proceedings from the Sensors for Nondestructive Testing International Conference*, Orlando, FL, pp. 324–342.
- Throop, J.A., Aneshansley, D.J., Anger, B., 1999. Inspection station detects defects on apples in real time. ASAE Paper No. 993205, ASAE, St. Joseph, MI, p. 49085.
- Throop, J.A., Aneshansley, D.J., Anger, B., 2000. Multispectral imaging station detects defects on apples. *Photonics East 2000. Conference 4203-Biological Quality and Precision Agriculture II*, November 7–8, 2000, Boston, MA.
- Throop, J.A., Aneshansley, D.J., Upchurch, B.L., Anger, B., 2001. Apple orientation on two conveyors: performance and predictability based on fruit shape characteristics. *Trans. ASAE* 44 (1), 99–109.
- Throop, J. A., Aneshansley, D.J., Anger, W.C., Peterson, D.L., 2003. Conveyor design for apple orientation. ASAE Paper 036123, ASAE, St. Joseph, MI, p. 49085.
- Tichy, O. J., 1988. Apple orienting device. US Patent No. 4746001. Commissioner of Patents and Trademarks, Washington, DC, p. 5.
- USDA Agricultural Marketing Service, 1997. United States Standards for Grades of Apples for Processing. Fruit and Vegetable Division, Fresh Products Branch.
- VanderSchoot, J., 1994. Orienting mechanism for orienting fruit, for example. EP 0 436 244 B1, European Patent Office.
- Yang, Q., 1996. Apple stem and calyx identification with machine vision. *J. Agric. Eng. Res.* 63, 229–236.